The Plant Cell, Vol. 10, 255–266, February 1998 © 1998 American Society of Plant Physiologists

A Plant Homolog of the Neutrophil NADPH Oxidase gp91^{phox} Subunit Gene Encodes a Plasma Membrane Protein with Ca^{2+} Binding Motifs

Thomas Keller,[a,b] Howard G. Damude,[a] Dietrich Werner,[b] Peter Doerner,[a] Richard A. Dixon,[c] and Chris Lamb[a,1]

[a] Plant Biology Laboratory, Salk Institute, La Jolla, California 92037
[b] Fachbereich Biologie, Philipps-Universität, 35032 Marburg, Germany
[c] Plant Biology Division, Noble Foundation, Ardmore, Oklahoma 73402

Rapid generation of O_2^- and H_2O_2, which is reminiscent of the oxidative burst in neutrophils, is a central component of the resistance response of plants to pathogen challenge. Here, we report that the Arabidopsis *rbohA* (*for respiratory burst oxidase homolog A*) gene encodes a putative 108-kD protein, with a C-terminal region that shows pronounced similarity to the 69-kD apoprotein of the gp91^{phox} subunit of the neutrophil respiratory burst NADPH oxidase. The RbohA protein has a large hydrophilic N-terminal domain that is not present in gp91^{phox}. This domain contains two Ca^{2+} binding EF hand motifs and has extended similarity to the human RanGTPase-activating protein 1. *rbohA*, which is a member of a divergent gene family, generates transcripts of 3.6 and 4.0 kb that differ only in their polyadenylation sites. *rbohA* transcripts are most abundant in roots, with weaker expression in aerial organs and seedlings. Antibodies raised against a peptide near the RbohA C terminus detected a 105-kD protein that, unlike gp91^{phox}, does not appear to be highly glycosylated. Cell fractionation, two-phase partitioning, and detergent extraction indicate that RbohA is an intrinsic plasma membrane protein. We propose that plants have a plasma membrane enzyme similar to the neutrophil NADPH oxidase but with novel potential regulatory mechanisms for Ca^{2+} and G protein stimulation of O_2^- and H_2O_2 production at the cell surface.

INTRODUCTION

Recognition of avirulent pathogens causes a burst of oxidative metabolism generating superoxide (O_2^-) and hydrogen peroxide (H_2O_2) (Baker and Orlandi, 1995). Reactive oxygen intermediates are direct protective agents and also drive cross-linking of the cell wall before the activation of transcription-dependent defenses (Lamb and Dixon, 1997). Moreover, the oxidative burst can trigger the collapse of challenged host cells at the onset of the hypersensitive response and generate signals for defense gene induction (Levine et al., 1994; Jabs et al., 1997).

The kinetics and defense functions of O_2^- and H_2O_2 generation are reminiscent of the oxidative burst during neutrophil activation (Tenhaken et al., 1995; Lamb and Dixon, 1997). The neutrophil oxidative burst involves the reaction $O_2 + NADPH \rightarrow O_2^- + NADP^+ + H^+$ catalyzed by a plasma membrane oxidase, followed by dismutation of O_2^- to H_2O_2 (Taylor et al., 1993). The NADPH oxidase consists of two plasma membrane proteins, gp91^{phox} and p22^{phox} (*phox* for phagocyte oxidase), which together form heterodimeric flavocytochrome b_{-558} and three cytosolic regulatory proteins, p40^{phox}, p47^{phox}, and p67^{phox}, which translocate to the plasma membrane after stimulation to form the active complex (Bokoch, 1994). The small cytosolic GTPase Rac2 and possibly other G proteins also appear to be required for activation of the oxidase.

A membrane-bound enzyme resembling the neutrophil NADPH oxidase may contribute to the pathogen-induced oxidative burst in plants. Thus, O_2^- generation can be observed in microsomal preparations (Doke, 1983a), protoplasts are able to generate an oxidative burst in response to avirulence signals (Doke, 1983b), and H_2O_2 accumulates in the inner region of the apoplast of infected leaf tissue (Bestwick et al., 1997). Diphenylene iodonium, which at micromolar concentrations is a suicide substrate inhibitor of the neutrophil NADPH oxidase, blocks the oxidative burst in plant cells with similar potency (Levine et al., 1994; Auh and Murphy, 1995; Dwyer et al., 1996; Jabs et al., 1997). Moreover, antibodies raised against human p22^{phox}, p47^{phox}, and p67^{phox} cross-react with appropriately sized polypeptides in plant extracts (Tenhaken et al., 1995; Desikan et al., 1996; Dwyer et al., 1996; Xing et al., 1997).

[1] To whom correspondence should be addressed. E-mail lamb@salk.edu; fax 619-558-6379.

Two rice expressed sequence tags (ESTs) encode short segments of predicted polypeptides with similarity to human gp91*phox*. From nucleotide sequencing of the partial cDNAs containing these ESTs and 4.3 kb of the corresponding *rbohA* (for *respiratory burst oxidase homolog A*) gene, an open reading frame (ORF) putatively encoding a 69-kD protein with pronounced similarity to the gp91*phox* apoprotein was recently described (Groom et al., 1996). However, no experimental data on the occurrence or properties of the deduced protein were presented, and the putative full-length cDNA and ORF, which were assembled by reference to the genomic sequence, were not verified by RNA hybridization or rapid amplification of cDNA ends (RACE).

Here, we describe an extended version of the rice *rbohA* cDNA and a full-length Arabidopsis homolog that encode predicted proteins with large hydrophilic N-terminal domains containing two Ca^{2+} binding EF hand motifs and have extended similarity to a human GTPase activating protein. We show that Arabidopsis *rbohA* generates transcripts of 3.6 and 4.0 kb, differing only in the site of polyadenylation, and that RbohA is a 108-kD intrinsic plasma membrane protein. These findings support the hypothesis that plant plasma membranes contain an enzyme system closely related to the neutrophil NADPH oxidase and reveal novel potential regulatory mechanisms for Ca^{2+} and G protein activation of the oxidative burst at the cell surface.

RESULTS

Rice and Arabidopsis gp91*phox* Homologs

By probing a rice cDNA library with the 390-bp EST cDNA RICR1901A (GenBank accession number D39082), we identified a clone (C1/1/1) containing a 2.8-kb insert. The ORF has 1865 bp that are identical to the *rbohA* gene sequence. However, it abruptly diverges 40 bp 3′ of the previously inferred translation start codon (Groom et al., 1996) to give an extended ORF that has an additional 374 bp upstream from the point of divergence to the 5′ terminus of the C1/1/1 clone, as shown in Figures 1A and 2 (see also GenBank accession number AFO15302).

Products from polymerase chain reaction (PCR) with Arabidopsis cell suspension cDNA templates and primers from the rice C1/1/1 sequence were used to screen an Arabidopsis cDNA library (Schindler et al., 1992). The longest Arabidopsis *rbohA* cDNA contained an ORF of 2835 bp within the 3.2-kb insert (Figure 1A, and see GenBank accession number AFO15301 for annotated Arabidopsis *rbohA* sequences), and 5′ RACE, as depicted in Figure 3, revealed an additional 308 bp upstream of the 5′ terminus of this clone (Figures 1 and 2). This extended sequence, which contained stop codons in all reading frames, was confirmed by sequencing a genomic subclone covering the 5′ RACE fragment. Thus, the first in-frame ATG of the Arabidopsis *rbohA* cDNA clone is the likely start codon, and the ensuing ORF encodes a protein of 944 amino acids with a predicted molecular mass of 108 kD (Figures 1 and 2, and GenBank accession number AFO15301).

The C-terminal region of the Arabidopsis RbohA protein and the truncated rice version show pronounced similarity to mammalian gp91*phox* (Royer-Pokora et al., 1986), with 32% amino acid sequence identity between gp91*phox* and the corresponding region of RbohA (Figure 2 and GenBank accession number AFO15301). As noted for rice RbohA (Groom et al., 1996), this sequence identity reflects conservation in the plant proteins of structural attributes contributing to gp91*phox* catalytic activity and topological organization, with a similar arrangement of six hydrophobic stretches likely to be transmembrane helices (Figures 1B and 2, and GenBank accession number AFO15301). Four sites in human gp91*phox* cooperate in the interaction with p47*phox* (De Leo et al., 1995,

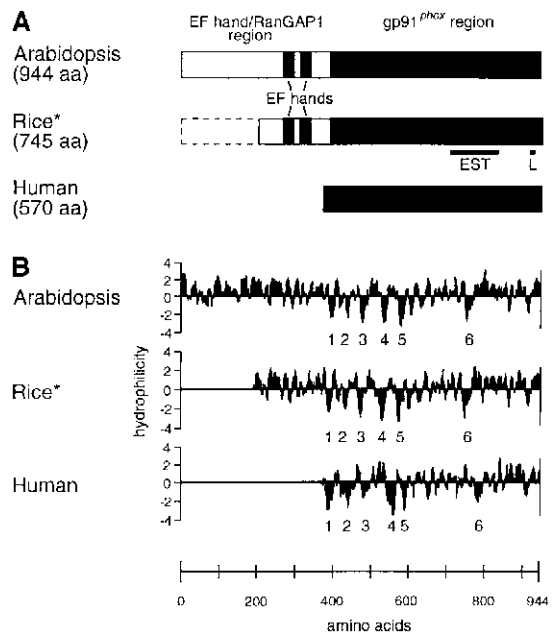

Figure 1. Structure and Hydrophilicity Plots of RbohA in Comparison with Human gp91*phox*.

(A) Size and structure of Arabidopsis and rice RbohA protein in comparison to human gp91*phox*. Unshaded area, N-terminal domain; black-shaded area, gp91*phox* region; black vertical bars, EF hand motifs; aa, amino acid; EST, region spanned by rice EST RICR 1901A; L, immunogen peptide. The asterisk denotes the 5′ truncated sequence.

(B) Hydrophilicity plots (Kyte and Doolittle, 1982) for the Arabidopsis and rice RbohA proteins in comparison to human gp91*phox*. The curves represent residue-specific hydrophilicity indices averaged from a moving nine-residue window. Increased hydrophobicity is indicated by negative values. The numbers 1 to 6 denote putative membrane-spanning domains.

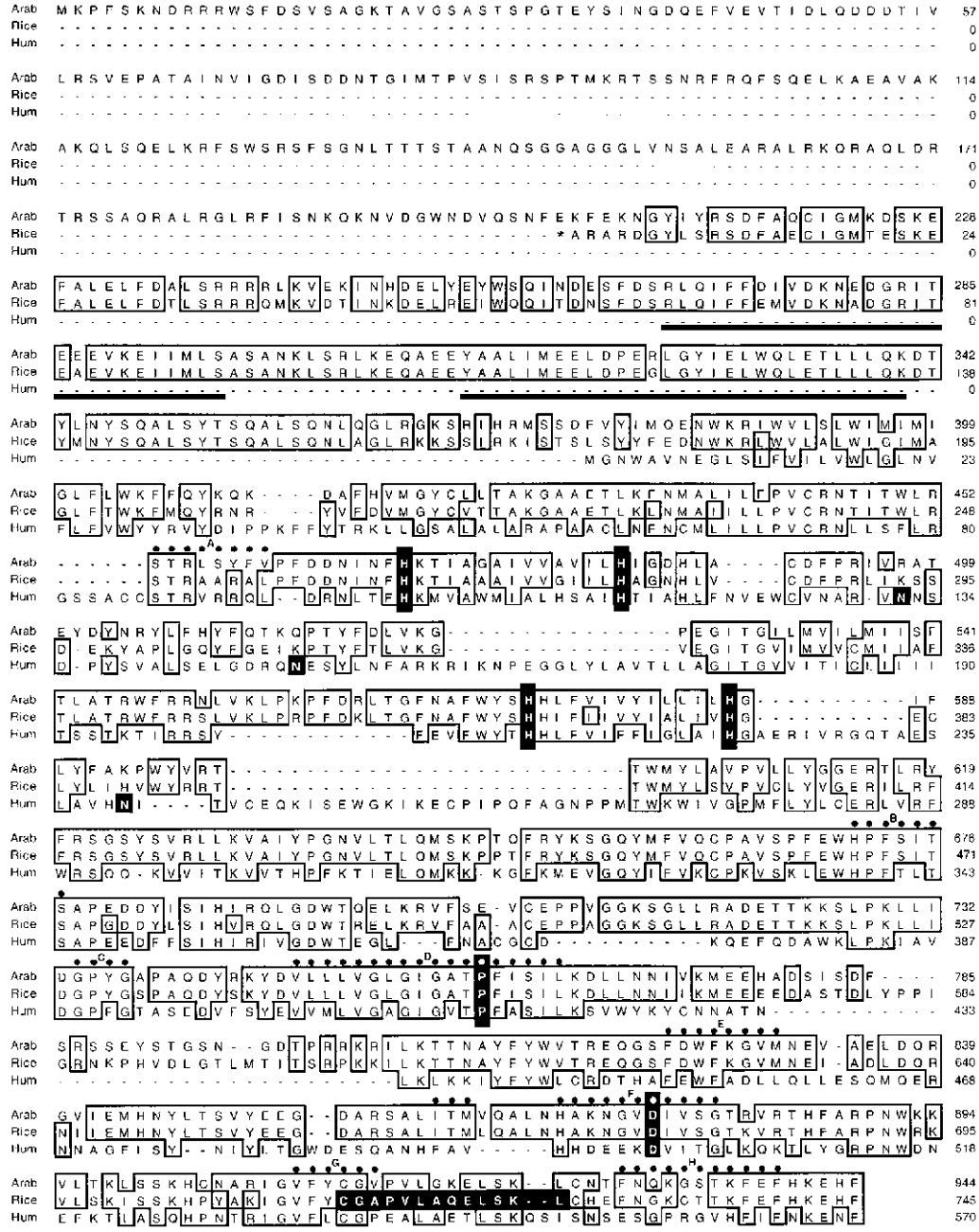

Figure 2. Amino Acid Sequence Alignments of Human gp91*phox* and the Deduced Arabidopsis and Rice RbohA Proteins.

Open boxes denote conserved amino acid residues. Dots above the residues denote residues in motifs implicated in human gp91*phox* enzyme function. A, E, F, and H are p47*phox* binding sites in the human gp91*phox* subunit. Nucleotide binding motifs identified in other oxidoreductases are B (FAD–isoalloxazine binding site), C (motif 2), D (NADPH–ribose binding site), and G (NADPH binding site). Histidine residues involved in heme binding, asparagine residues involved in N-glycosylation, proline-415 and aspartate-500 of human gp91*phox*, and the corresponding residues in RbohA, where conserved, as well as peptide L, are indicated by white letters on a black background. EF hand motifs are underlined. Dashes denote gaps introduced to optimize alignment. The asterisk indicates truncation of the cloned sequence. Arab, Arabidopsis; Hum, human.

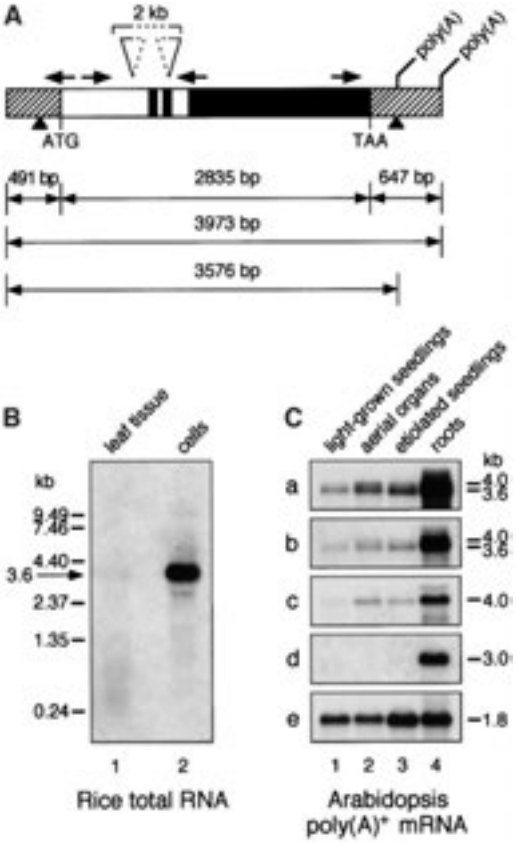

Figure 3. *rbohA* Transcripts.

(A) Structure of Arabidopsis *rbohA* transcripts. Hatched areas denote untranslated regions; unshaded and shaded areas are as given in Figure 1. Solid arrowheads denote the termini of the 3.2-kb cDNA clone; arrows denote locations and orientations of PCR primers. The 5′ splice site and 3′ splice site, respectively, of two introns identified by sequencing the product from PCR amplification of the corresponding 2.0-kb genomic sequence are indicated by inserts at top (solid lines denote sequenced regions).

(B) RNA gel blot hybridization of rice *rbohA* transcripts. Total RNA (20 μg) from leaves (lane 1) and cell suspension cultures (lane 2) was hybridized with a 711-bp fragment derived from rice *rbohA* cDNA C1/1/1.

(C) RNA gel blot hybridization of Arabidopsis *rbohA* and *rbohB* transcripts. Poly(A)$^+$ RNA (1 μg per lane) was purified from 5-day-old light-grown seedlings (lane 1), aerial organs of 13-day-old plants (lane 2), 8-day-old etiolated seedlings (lane 3), and roots of 13-day-old plants (lane 4). Blot a was probed with a 2.3-kb *rbohA* cDNA; blot b with a 288-bp PCR fragment spanning the EF hand region; blot c with a strand-specific fragment of the 3′ untranslated region unique to the longer transcript; blot d with a 250-bp gene-specific fragment of *rbohB*; and blot e with constitutively expressed *eIF-4A* as a control for RNA loading.

In **(B)** and **(C)**, numbers at left and right, respectively, indicate transcript sizes in nucleotides, calculated by interpolation from coelectrophoresed size markers. In **(B)**, the arrow points to the rice *rbohA* transcript.

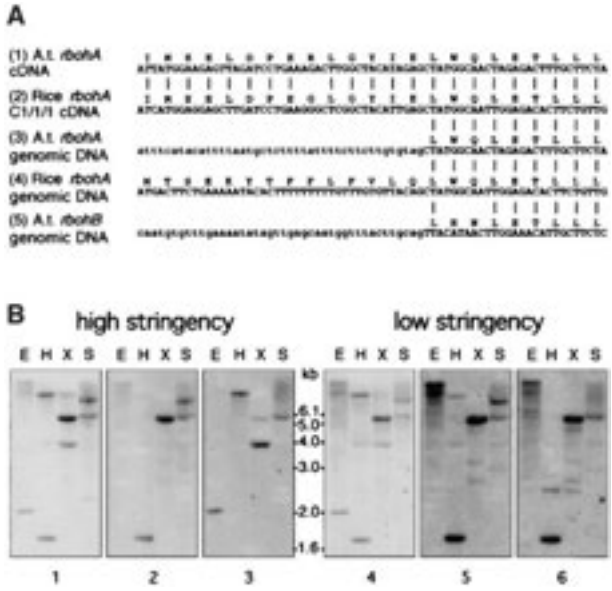

Figure 4. Arabidopsis *rbohA* Gene Organization.

(A) Comparison of the Arabidopsis (A.t.) *rbohA* cDNA (1) and gene (3) sequences and the rice *rbohA* C1/1/1 cDNA sequence (2) from this study with the rice gene sequence in the region of the translation initiation codon previously proposed for *rbohA* ([4]; Groom et al., 1996) and the Arabidopsis *rbohB* gene sequence ([5]; GenBank accession number ACO00106). Vertical bars denote identical amino acid residues; lowercase letters denote nucleotides in intron sequences.

(B) DNA gel blot hybridization. Arabidopsis genomic DNA digested with EcoRI (E), HindIII (H), XbaI (X), or SphI (S) was hybridized with *rbohA* sequences as follows: lanes 1 and 4, 3.2-kb cDNA; lanes 2 and 5, 1.68-kb cDNA fragment spanning the gp91^{phox} region; lane 3, 1.26-kb cDNA spanning the EF hand/RanGAP1 region; lane 6, 0.6-kb cDNA spanning a highly conserved stretch of the gp91^{phox} region, at high (lanes 1 to 3) and low (lanes 4 to 6) stringency. Numbers at center are fragment sizes in kilobases from coelectrophoresed markers.

1996). Several residues in these binding sites are conserved in both Arabidopsis and rice RbohA (Figure 2), suggesting that the plant proteins interact with a similar cytosolic regulatory component. In addition, features required for the catalytic function of neutrophil gp91^{phox} are also conserved in the plant proteins. Thus, potential motifs involved in NADPH and flavin binding of human gp91^{phox} (Segal et al., 1992; Taylor et al., 1993) are also present in both plant homologs. Likewise, four histidine residues (His-101, His-115, His-209, and His-222), which are important for heme binding in yeast ferric reductase and human gp91^{phox}, are conserved in both the Arabidopsis and rice RbohA proteins (Finegold et al., 1996). Moreover, gp91^{phox} amino acid residues Pro-415 and Asp-500 are also conserved in both Arabidopsis and rice

RbohA. Substitution of Pro-415 by a histidine residue and Asp-500 by a glycine residue inactivates NADPH oxidase, resulting in chronic granulomatous disease (Segal et al., 1992).

RbohA Contains a Large Hydrophilic N-Terminal Domain with Two EF Hand Motifs and Extended Sequence Similarity to RanGAP1

The Arabidopsis *rbohA* cDNA and the rice C1/1/1 version contain ORFs encoding substantially larger proteins than that inferred from rice *rbohA* genomic sequences (Groom et al., 1996). PCR with a primer from the extended N-terminal region and a primer close to the junction of this region and the gp91*phox* region (Figure 3A) generated the predicted 627-bp product from the cDNA template but a 2.0-kb product with Arabidopsis genomic DNA (Figure 3A). As shown in Figure 4A, the nucleotide sequence of the 3′ region of this genomic PCR product revealed an intron located exactly at the point of abrupt divergence of the Arabidopsis and rice *rbohA* cloned cDNA sequences from the ORF inferred from the rice *rbohA* genomic sequence (Groom et al., 1996).

Overall, the deduced amino acid sequence of the rice C1/1/1 *rbohA* cDNA shows 77% identity to the corresponding sequence in Arabidopsis *rbohA.* This sequence conservation not only is observed in the gp91*phox* region but also extends throughout the novel N-terminal region, which is very hydrophilic and has no candidate membrane-spanning domains (Figures 1B and 2). As shown in Figure 5, motif searches revealed two EF hand motifs located 50 to 122 amino acids from the beginning of the gp91*phox* region (Figures 1 and 2). Both RbohA EF hand motifs conform to the canonical sequence motif, including an invariant glycine, residues that are preferentially glutamate (−Z in canonical sequence in Figure 5), isoleucine (I in canonical sequence), and hydrophobic residues (n in canonical sequence) at specific positions within a predicted helix-loop-helix structure characteristic of EF hands (Figure 5). These putative Ca^{2+} binding motifs are located in a tract that is highly conserved in the Arabidopsis and rice RbohA proteins (93% amino acid identity). The two EF hand motifs are separated by 15 amino acids, and both motifs span 29 amino acids. The EF hand motifs in RbohA are most similar to the first Ca^{2+} binding domain of the birch pollen allergen *Bet v* III (Seiberler et al., 1994) (Figure 5) and more distantly related to EF hand motifs in other Ca^{2+} binding proteins, such as the touch-induced calmodulin-related protein 2 of Arabidopsis (Braam and Davis, 1990).

In addition, as shown in Figure 6, RbohA exhibits extended similarity to the human RanGTPase-activating protein 1 (RanGAP1), which is the GTPase activator for the Ras-related G protein Ran promoting conversion of Ran to a GDP-bound inactive form (Bischoff et al., 1995). When the whole N-terminal domain of RbohA is considered, there is 23% identity with human RanGAP1, and the 64–amino acid stretch between residues 113 and 177 of RbohA shows 40% identity to the corresponding region of RanGAP1. Ten of 25 conserved leucine residues, which appear to play important functions in the RanGAP protein family in animals and yeast, are also found in Arabidopsis RbohA, including those in the motif LxxxxLxDNxF (where x stands for any amino acid residue), which occurs twice in RanGAP homologs (Figure 6 and GenBank accession number AFO15301). RbohA is unrelated to the GTPase activators for other Ras-related proteins.

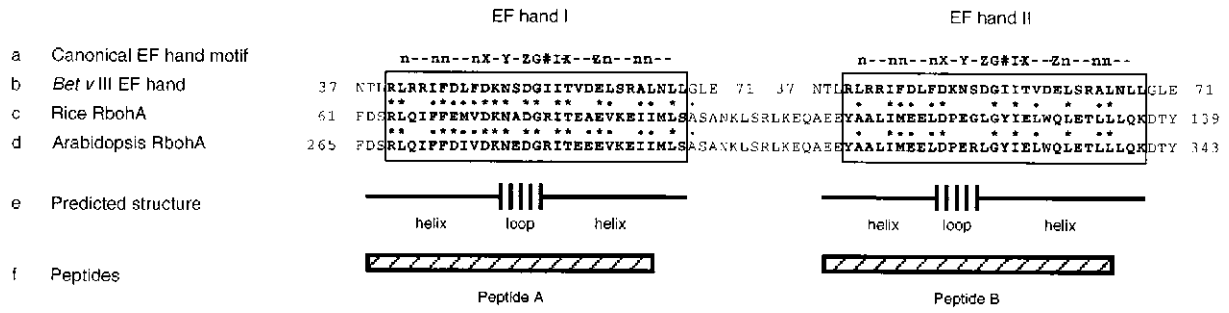

Figure 5. EF Hand Motifs in the N-Terminal Domain of RbohA.

Amino acid sequence alignment of two EF hand motifs in Arabidopsis RbohA and the truncated version from rice with the canonical EF hand motif and the first Ca^{2+} binding domain of the birch pollen allergen *Bet v* III are shown. a, canonical EF hand motif (Kretsinger, 1996); b, *Bet v* III EF hand motif (Seiberler et al., 1994); c, rice RbohA N-terminal partial sequence; d, Arabidopsis RbohA N-terminal partial sequence; e, predicted helix-loop-helix organization of EF hand motifs I and II of Arabidopsis RbohA; f, peptides synthesized for Ca^{2+} binding studies. Boxes define the consensus EF hand region; asterisks and dots denote identical and similar amino acid residues, respectively; n, usually hydrophobic amino acid residues; dashes indicate variable (often hydrophilic) amino acid residues; X, Y, Z, −X, oxygen atoms or bridging water molecules of side chains of this amino acid residue coordinate Ca^{2+}; G, invariant amino acid residue Gly; #, carbonyl oxygen of this amino acid residue serves as ligand; I in canonical EF hand motif represents Ile, Leu, or Val; −Z, usually Glu.

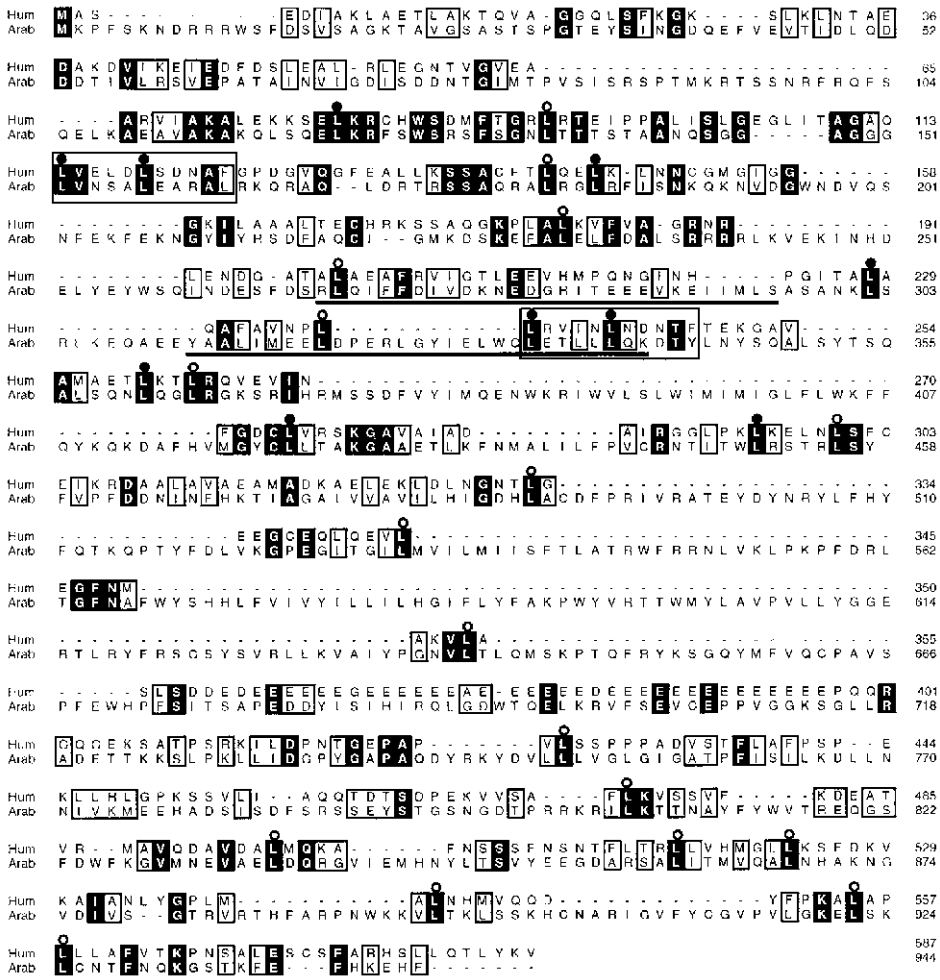

Figure 6. Arabidopsis RbohA Shows Extended Sequence Similarity to Human RanGAP1.

Black and white boxes denote identical and similar residues, respectively. Large boxes denote the LxxxxLxDNxF motif found twice in animal RanGAP1-related proteins. Closed circles indicate the 10 leucine residues that are conserved in animal and yeast RanGAP homologs and Arabidopsis (Arab) RbohA; open circles denote additional leucine residues conserved between human (Hum) RanGAP1 and Arabidopsis RbohA. EF hand regions are underlined; dashes indicate gaps introduced to optimize alignment.

Gene Organization

Gel blot hybridizations were performed with Arabidopsis genomic DNA samples digested separately using four restriction enzymes that each have a single restriction site in the 3.2-kb Arabidopsis *rbohA* cDNA. High-stringency hybridization with this cDNA resulted in each case in the detection of two major restriction fragments (Figure 4B). Moreover, when these blots were hybridized separately with probes spanning the EF hand/RanGAP1 region and the gp91^{phox} region, single restriction fragments were detected with each probe–restriction enzyme combination, except for the SphI digest hybridized with the gp91^{phox} region probe, in which two fragments were detected because of an internal SphI site (Figure 4B). Weak hybridization of the EF hand/RanGAP1 region probe to a XbaI fragment of ~6 kb corresponds to a single fragment of the same length that strongly hybridized with the gp91^{phox} region probe. Overall, the high-stringency hybridization patterns with the EF hand/RanGAP1 region and gp91^{phox} region as probes complement each other and together account for the hybridization pattern with the *rbohA* cDNA as probe. These simple patterns reflect hybridization with a single gene that maps near the bottom of chromosome 1 and is 5.6 centimorgans distal to g4026 and 3.6 centimorgans proximal to m315. Its location is adjacent to *NPR1*, which functions in the expression of induced resis-

tance (Cao et al., 1997). These mapping data were derived from segregation analysis of restriction fragment length polymorphisms in 28 recombinant inbred lines (Lister and Dean, 1993).

The high-stringency hybridizations allowed only ~9% mismatch, and hence the Arabidopsis genome does not contain any very closely related sequences. However, recently, bacterial artificial chromosome clone F7G19 (GenBank accession number ACO00106) containing Arabidopsis genomic DNA from the upper arm of chromosome 1 was sequenced, enabling us to identify a gene that, with assumptions about likely splice sites, generates an ORF encoding another gp91^{phox} homolog with an extended N-terminal domain containing EF hand motifs. The sequence of this gene, which we designate *rbohB*, was only ~65% similar to that of *rbohA.* By probing DNA gel blots at low stringency, allowing ~30% mismatch, we identified several weakly hybridizing bands (Figure 4B). None of these bands corresponded to restriction fragments predicted from the *rbohB* sequence. Therefore, the Arabidopsis genome may contain, in addition to *rbohA* and *rbohB*, several other highly divergent genes encoding homologs of gp91^{phox}.

rbohA Transcripts

On gel blots of total RNA from rice cell suspensions, a single ~3.6-kb transcript was hybridized with *rbohA* C1/1/1 cDNA (Figure 3B), whereas no hybridization was observed on blots of total RNA from rice leaves (Figure 3B) or Arabidopsis plants (data not shown). This suggests a low abundance in plant tissues. Therefore, *rbohA* transcripts were analyzed in poly(A)$^+$ RNA purified from total RNA extracts of Arabidopsis seedlings and young plants. Transcripts of 3.6 and 4.0 kb were hybridized with the 2.3-kb *rbohA* cDNA and also with a 288-bp fragment from the EF hand region (Figure 3C). 3′ RACE with a primer 347 bp upstream of the 3′ terminus of the 3.2-kb *rbohA* cDNA (113 bp 5′ of the terminus of the ORF) generated two products of 404 and 784 bp, with 366 bp of overlapping identical sequences (Figure 3A). A strand-specific fragment from the nonoverlapping region of the 3′ terminus of the 4.0-kb transcript did not hybridize with the shorter transcript (Figure 3C). Both transcripts contained a poly(A) tail, and we conclude that *rbohA* transcription generates a single mRNA with two different polyadenylation sites. The ratio of the 4.0-kb transcript and more abundant 3.6-kb transcript was similar in all samples tested. The greatest accumulation of *rbohA* transcripts was observed in roots of 13-day-old plants, with weaker expression in the aerial organs of these plants and in seedlings (Figure 3C). In contrast, a gene-specific probe for *rbohB* hybridized with a 3.0-kb transcript found only in root poly(A)$^+$ RNA (Figure 3C). A number of defense-related genes exhibit preferential expression in roots, possibly as a protection against continual wounding and high disease pressure as roots grow through the soil (Lamb et al., 1989).

RbohA Is an Intrinsic Plasma Membrane Protein

Antisera raised against a conserved peptide, designated L, located near the C terminus (Figure 1) reacted with a 97-kD protein in rice cell extracts and a 105-kD protein in Arabidopsis cell extracts, as shown by protein gel blot analysis illustrated in Figure 7. The estimated molecular mass of 105 kD for the immunoreactive Arabidopsis protein was in good agreement with the molecular mass of 108 kD deduced from the complete ORF of the cDNA clone. In contrast to the strong conservation of amino residues important for the catalytic function and regulation of gp91^{phox}, three glycosylation sites (Asn-132, Asn-149, and Asn-240) in human gp91^{phox} (Wallach and Segal, 1997) are not conserved in the plant RbohA proteins (Figure 2), and unlike gp91^{phox}, RbohA does not appear to be extensively glycosylated. Moreover, whereas slower migrating species were occasionally detected with the anti-L serum, they were not glycosylated forms of RbohA because chemical and enzymatic deglycosylation treatments had no effect on their electrophoretic

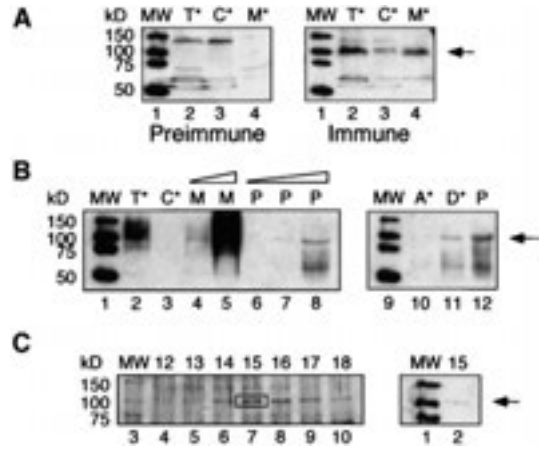

Figure 7. Size, Cellular Localization, and Purification of RbohA.

(A) Protein gel blots of fractionated rice cell extracts probed with preimmune serum or anti-L antiserum.

(B) Protein gel blots of fractionated Arabidopsis cell extracts probed with anti-L antiserum. Gradients denote progressive increases in protein loadings.

(C) RbohA purification. Shown at left are silver-stained SDS–polyacrylamide gels of the fractions collected from Superdex gel filtration. The box denotes the purified RbohA equivalent to that used for N-terminal sequencing. At right is the protein blot analysis of this fraction.

Protein loading of gels is given as follows: **(A)** lanes 2 to 4 (both gels), 73, 64, and 17 μg, respectively; **(B)** lanes 2 to 8, 40, 31, 6.4, 64, 0.25, 2.5, and 25 μg, respectively; lanes 10 and 11, not determined; lane 12, 25 μg. Lanes 10 and 11 and all samples marked with an asterisk above were loaded on a cell-equivalent basis. In **(B)**, the cell equivalent loading for P would be 9 μg. Arrows denote RbohA. A, aqueous phase; C, cytosolic supernatant; D, detergent phase; M, microsomes; MW, molecular mass markers; P, plasma membrane; T, total cell protein.

mobilities. Simultaneous treatments of native gp91^{phox} significantly increased its mobility (data not shown). These species were almost entirely eliminated when less protein was loaded on the gel (e.g., compare lanes 4, 5, and 7 in Figure 7B) and hence appear to be aggregated forms. In rice extracts, immunoreactive RbohA always appeared as a discrete band with no aggregation. Bands at ~140 and ~60 kD, which reacted weakly with the immune serum, were also observed with the preimmune serum and hence do not appear to be RbohA-related species.

Rice RbohA was predominantly microsomal, with substantially less immunoreactivity in the cytosolic fraction (Figure 7A). Arabidopsis RbohA was found almost exclusively in the microsomal fraction. Fractionation of Arabidopsis microsomes by two-phase partitioning showed that RbohA partitioned into the polyethylene glycol phase (Figure 7B), which was 180-fold enriched relative to the dextran phase for the plasma membrane marker β-1,3-glucan synthase. Moreover, Triton X-114 extraction of this purified plasma membrane fraction resulted in the partitioning of RbohA predominantly in the detergent phase (Figure 7B), indicating that RbohA is a large intrinsic plasma membrane protein. Immunoreactive proteins of 60 to 80 kD appearing in purified plasma membrane fractions most likely reflect partial degradation of RbohA at low overall protein concentrations in the later stages of cell fractionation, because species of this size were not detected in whole-cell extracts or microsomes (Figure 7).

RbohA Purification and N Terminus

Immunoreactive RbohA was purified from Arabidopsis cell suspension cultures by ion exchange chromatography, gel filtration, and electrophoresis (Figure 7C). Purification was monitored by immunoreactivity with the anti-peptide L antiserum in protein gel blots, and the identity of the purified protein was confirmed with an antibody raised against a second peptide comprising the final 10 residues at the C terminus of the deduced RbohA protein (data not shown). Only a small amount of purified RbohA was obtained for N-terminal sequence analysis, but the first two amino acids were shown to be lysine and proline, which are the first two amino acids encoded immediately downstream of the first in-frame ATG of the *rbohA* cDNA ORF (Figure 2).

RbohA EF Hand Motifs Bind Ca^{2+}

Protein gel blot analysis and N-terminal sequencing of native RbohA demonstrated that the novel N-terminal domain deduced from *rbohA* cDNA sequences is indeed present in the mature RbohA protein. To initiate functional analysis of the N-terminal domain, we tested whether the EF hand motifs had the capacity to bind Ca^{2+}. As shown in Figure 8, immobilized synthetic versions of both Arabidopsis RbohA EF hand motifs bound $^{45}Ca^{2+}$, whereas negligible binding was observed with peptide L as a negative control for background. Moreover, there was only very weak Ca^{2+} binding to a scrambled version of the EF hand motif I sequence (Figure 8). Thus, binding to the RbohA EF hand motifs does not simply reflect nonspecific binding to peptides that are relatively rich in acidic amino acid residues but is dependent on the specific structure of the EF hand motif.

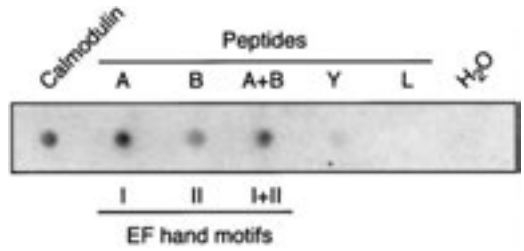

Figure 8. $^{45}CaCl_2$ Binding to Immobilized Arabidopsis RbohA EF Hand Motifs.

$^{45}CaCl_2$ binding to the indicated peptides (4 μg), with spinach calmodulin (0.4 μg) as a positive control, was monitored by autoradiography. Peptides A and B are synthetic versions of the Arabidopsis EF hand motifs I and II, respectively (see Figure 5). Peptide Y, which is a scrambled version of the Arabidopsis EF hand motif I sequence, and peptide L were negative controls.

EF hand motif I, which more closely resembles the EF hand consensus motif, bound Ca^{2+} more strongly than did EF hand motif II. $^{45}Ca^{2+}$ binding to the EF hand motifs was competed >90% with 1000-fold excess $^{40}CaCl_2$, but not by an equivalent excess of $FeCl_2$ (data not shown). Ca^{2+} binding was not enhanced by mixing the two peptides and was weaker than binding to EF hand motifs in the context of native spinach calmodulin (Figure 8), which is consistent with a contribution to EF hand motif activity from macromolecular interactions.

DISCUSSION

Several lines of evidence indicate that Arabidopsis *rbohA* encodes a protein substantially larger than either the apoprotein of gp91^{phox} or that previously inferred from rice *rbohA* genomic sequences. Thus, the extended ORF encoding the novel N-terminal domain is also found in the rice C1/1/1 *rbohA* cDNA clone, and *rbohA* transcripts of ⩾3.6 kb were observed in both Arabidopsis and rice extracts. Moreover, the Arabidopsis 3.2-kb cDNA clone contains a full-length ORF, and the 3.6- and 4.0-kb transcripts are fully accounted for by the 5′ RACE extension and the respective 3′ RACE extensions. Likewise, antiserum raised against a conserved peptide near the RbohA C terminus detected proteins of 97 kD in rice and 105 kD in Arabidopsis. The latter is in excellent agreement with the molecular mass deduced

from the full-length ORF and in keeping with the absence of extensive glycosylation. Moreover, a full-length protein, which contained the predicted first two residues at the N terminus and was immunoreactive with antibodies raised against peptides adjacent to the C terminus, was recovered from Arabidopsis microsomes, indicating that the native plasma membrane protein comprises the entire product encoded by the *rbohA* ORF.

RNA gel blot hybridizations did not reveal a smaller transcript that might carry an ORF spanning the gp91^{phox} region but not the N-terminal region. Likewise, no evidence for the corresponding ~70-kD apoprotein was observed on protein gel blots of total cell extracts or microsomal fractions, even though the antiserum was raised against a conserved peptide near the C terminus of the gp91^{phox} region. An intron in the Arabidopsis *rbohA* gene, in a sequence highly conserved in rice *rbohA*, is located precisely at the point of divergence of the rice C1/1/1 cDNA and *rbohA* gene sequences. Conservation of this intron location in the rice *rbohA* gene would account for the apparently truncated ORF inferred from this gene sequence (Groom et al., 1996). Because Arabidopsis *rbohB* apparently also encodes a protein with an extended N-terminal region similar to that in RbohA, there is at present no experimental evidence for plant gp91^{phox} homologs lacking this region. It will be of interest to determine whether other members of this highly divergent plant gene family encode proteins with a truncated N terminus as is found in gp91^{phox}.

RbohA is much more similar to human gp91^{phox} than to ferric reductase (Groom et al., 1996), a related enzyme that transfers electrons across cell membranes to Fe^{3+} as the terminal acceptor. The observation that RbohA is an intrinsic plasma membrane protein with striking similarity to neutrophil gp91^{phox} strongly suggests that plants also have an NADPH oxidase for the rapid generation of reactive oxygen intermediates at the cell surface (Lamb and Dixon, 1997). Further support for this conclusion comes from the observation that expression of *rbohA* antisense constructs in transgenic Arabidopsis compromises the hypersensitive response (W. Aufsatz, T. Keller, H.G. Damude, P. Doerner, R.A. Dixon, and C. Lamb, unpublished observations). The apparent conservation of membrane topology between gp91^{phox} and RbohA means that the initial products of the NADPH oxidase reaction will accumulate on the external face of the plasma membrane (Bestwick et al., 1997), in keeping with the functions of reactive oxygen intermediates in wall cross-linking and intercellular signaling (Lamb and Dixon, 1997).

The extended N-terminal domain of RbohA provides novel potential regulatory mechanisms for activation of the oxidative burst. The truncated N terminus in human gp91^{phox} is on the cytosolic side of the plasma membrane (A. Cross, personal communication). The apparent topological conservation between human gp91^{phox} and plant RbohA, together with the absence of hydrophobic stretches in the RbohA N-terminal domain, strongly suggest that this extended domain projects into the cytosol. Avirulence factors stimulate a rapid elevation of cytosolic Ca^{2+} (Knight et al., 1991), which plays a central role in the activation of defense responses (Mehdy, 1994; Baker and Orlandi, 1995; Bush, 1995; Jabs et al., 1997). In neutrophils, phosphorylation of p47^{phox} by protein kinase C helps to activate NADPH oxidase (Bokoch, 1994). Because a putative p47^{phox} has been immunologically detected in plant cell extracts (Xing et al., 1997) and binding sites for p47^{phox} are conserved in RbohA, Ca^{2+}-dependent protein phosphorylation may likewise contribute to the activation of NADPH oxidase in plants. However, the strong Ca^{2+} binding by the EF hand motifs in the RbohA N-terminal region provides a potential mechanism for direct regulation by Ca^{2+}. Unlike neutrophil gp91^{phox}, the thyroid plasma membrane NADPH-dependent H_2O_2 generator involved in thyroid hormone synthesis is directly regulated by Ca^{2+} (Gorin et al., 1997). It will be interesting to determine whether this enzyme has a similar structure to RbohA.

In plant disease resistance, direct activation of RbohA by Ca^{2+} may be important for rapid stimulation of the oxidative burst in challenged cells to prime the hypersensitive response (Lamb and Dixon, 1997; Shirasu et al., 1997). Moreover, because the cellular distribution of Ca^{2+} is highly compartmentalized (Knight et al., 1991; Bush, 1995), Ca^{2+} binding to RbohA may also provide spatial control for localized generation of reactive oxygen intermediates immediately adjacent to sites of attempted pathogen ingress (Bestwick et al., 1997).

Various G proteins function in the activation of the neutrophil NADPH oxidase (Bokoch, 1994). Pharmacological studies have implicated G proteins in the plant oxidative burst (Mehdy, 1994; Lamb and Dixon, 1997), and several disease resistance genes encode leucine-rich repeat proteins with putative nucleotide binding sites (Hammond-Kosack and Jones, 1997). The sequence similarity to RanGAP1 in the N-terminal region of RbohA suggests a possible mechanism for the attenuation of G protein signaling. Regulation of the magnitude and duration of the oxidative burst appears to be important in determining whether the response is restricted to wall cross-linking and local defense gene activation or progresses to threshold triggering of hypersensitive cell death (Levine et al., 1994; Lamb and Dixon, 1997). Moreover, transient activation of the oxidative burst can lead to a refractory period in which the signal system becomes insensitive to further stimulation (Legendre et al., 1993), and interplay between Ca^{2+} activation of RbohA and GTPase-mediated signal damping may contribute to stringent regulation of the NADPH oxidase.

METHODS

Plant Material

Arabidopsis (*Arabidopsis thaliana* ecotype Columbia) cell suspensions were initiated from root callus and cultured in Murashige and

Skoog (1962) medium containing 0.75 mg/L 2,4-dichlorophenoxyacetic acid and 0.35 mg/L benzyladenine. Arabidopsis and rice (*Oryza sativa* cv IR72; Zhu et al., 1995) cells were harvested 7 to 9 days after subculture. Plants were grown at 22°C under a 16-hr-light/8-hr-dark cycle or in continuous darkness.

Gel Blot Hybridization

Poly(A)$^+$ mRNA was purified from total cellular RNA by using Poly-A-Tract mRNA Isolation System IV (Promega, Madison, WI). Gel blots were hybridized at 60°C and washed twice at 60°C in 0.2 × SSC (1 × SSC is 0.15 M NaCl and 0.015 M sodium citrate) and 1% SDS. RNA loading was checked by hybridization with eukaryotic translation initiation factor 4A (*eIF-4A*) transcripts. Gel blots of Arabidopsis (ecotype Columbia) genomic DNA (10 μg) were hybridized at 55°C (low stringency) or 65°C (high stringency) for 24 hr in Church buffer (Sambrook et al., 1989). Probes were labeled with phosphorus-32 by random priming (Sambrook et al., 1989). Finally, the membranes were washed twice with 2 × SSC and 1% SDS at 60°C (low stringency) or 0.2 × SSC and 1% SDS at 65°C (high stringency).

rbohA Clones

Hybridization screening of rice bacterial artificial chromosome genomic (Wang et al., 1995) and λZapII (Stratagene, La Jolla, CA) cDNA (S. McCouch, Cornell University, Ithaca, NY) libraries and Arabidopsis genomic (J. Mulligan and R. Davis, Stanford University, Palo Alto, CA) and λZapII cDNA (Schindler et al., 1992) libraries, clone purification, subcloning, and nucleotide sequencing were performed using standard techniques (Sambrook et al., 1989). Deduced amino acid sequences were compared with protein and motif sequence databases by using BLAST (Altschul et al., 1990). The Arabidopsis and rice *rbohA* sequences have GenBank accession numbers AFO15301 and AFO15302, respectively.

Rapid Amplification of cDNA Ends

Rapid amplification of cDNA ends (RACE) systems (Gibco BRL, Gaithersburg, MD) were used with 0.5 μg of poly(A)$^+$ mRNA from Arabidopsis roots. Gene-specific primer 87 (5′-GTCGGAATTCAAAGAGTTGGTTGAAGGATATCGG-3′) and the poly(dT) adapter primer were used for 5′ and 3′ cDNA synthesis, respectively. cDNA (poly[dC] tailed for 5′ RACE) was then subjected to 35 (5′) and 20 (3′) polymerase chain reaction (PCR) cycles, respectively, using an annealing temperature of 55°C. The 50-μL PCR reaction contained 20 mM Tris-HCl, pH 8.4, 50 mM KCl, 1.5 mM $MgCl_2$, 0.4 μM nested gene-specific primer 88 (5′-GGAGAGATGGAGAATTGAAACGCG-3′) for 5′ RACE and primer 83 (5′-GAATAGGAGTGTTTTATTGCGGAGTACCGG-3′) for 3′ RACE, 0.4 μM abridged anchor primer, and 2.5 units of AmpliTaq polymerase (Perkin-Elmer, Branchburg, NJ). The PCR products were cloned into pGEM-T (Promega) for sequencing.

Antisera

Peptide L (CGAPVLAQELSKL) and the C-terminal peptide (TKFEFHKEHF) were made using an Applied Biosystems (Foster City, CA) synthesizer. Cleaved, deprotected peptides were conjugated through the N-terminal cysteine residue to keyhole limpet hemocyanin by using *N*-maleimidobenzoyl-*N*-hydroxysuccinimide ester (Harlow and Lane, 1988) and used to immunize rabbits at 3-week intervals.

Cell Fractionation

Whole-cell extracts (Zhu et al., 1995) were centrifuged twice at 10,000*g* for 10 min and then at 100,000*g* for 1 hr to give microsomal and cytosolic fractions. The distribution of β-1,3-glucan synthase was used to monitor plasma membrane purification from microsomes by partitioning in an aqueous polymer two-phase system (Larsson et al., 1987). Intrinsic and peripheral plasma membrane proteins were separated by Triton X-114 extraction (Justice et al., 1995). The size and cellular distribution of RbohA were determined by protein blotting (Sambrook et al., 1989).

N-Terminal Sequencing

Microsomal proteins dissolved in 50 mM potassium phosphate, 150 mM NaCl, 5 mM EDTA, and 0.75% CHAPS were centrifuged at 100,000*g* for 1 hr, and the supernatant was passed over a Hitrap SP (Pharmacia, Piscataway, NJ) cation exchanger. Flow-through was exchanged with 50 mM Tris-HCl, pH 8.0, and passed through a Q-Sepharose (Pharmacia) anion exchanger. Bound proteins were eluted with a gradient of NaCl (0 to 1 M), and fractions containing immunoreactive RbohA were concentrated and gel filtered through Superdex 200 (Pharmacia). Fractions containing RbohA were analyzed by SDS-PAGE with silver staining. The N-terminal sequence of 0.1 μg of purified RbohA was determined using an Applied Biosystems sequencer.

Ca^{2+} Binding

Peptides immobilized on nitrocellulose were incubated with 0.93 mM $^{45}CaCl_2$ (1 mCi/L; Amersham Life Science, Arlington Heights, IL) in a buffer containing 60 mM KCl, 5 mM $MgCl_2$, and 10 mM Mes, pH 5.5, for 10 min (Maruyama et al., 1984). After extensive washing, binding to the membranes was visualized by autoradiography.

ACKNOWLEDGMENTS

We thank Tsegaye Dabi for technical assistance and Jill Meisenhelder for peptide synthesis. T.K. and H.G.D. were supported by fellowships from the Evangelische Studienstiftung Haus Villigst, Schwerte, Germany, and the Natural Sciences and Engineering Research Council, Ottawa, Ontario, Canada, respectively. This research was supported by a grant to C.L. from the Samuel Roberts Noble Foundation.

Received October 10, 1997; accepted December 17, 1997.

REFERENCES

Altschul, S.F., Gish, W., Miller, W., Myers, E.W., and Lipman, D.J. (1990). Basic local alignment search tool. J. Mol. Biol. **215,** 403–410.

Auh, C.-K., and Murphy, T.M. (1995). Plasma membrane redox enzyme is involved in the synthesis of O_2^- and H_2O_2 by *Phytophthora* elicitor-stimulated rose cells. Plant Physiol. **107,** 1241–1247.

Baker, C.J., and Orlandi, E.W. (1995). Active oxygen in plant pathogenesis. Annu. Rev. Phytopathol. **33,** 299–321.

Bestwick, C.S., Brown, I.R., Bennett, M.H.R., and Mansfield, J.W. (1997). Localization of hydrogen peroxide accumulation during the hypersensitive reaction of lettuce cells to *Pseudomonas syringae* pv *phaseolicola.* Plant Cell **9,** 209–221.

Bischoff, F.R., Krebber, H., Kempf, T., Hermes, I., and Ponstingl, H. (1995). Human RanGTPase-activating protein RanGAP1 is a homologue of yeast Rna1p involved in mRNA processing and transport. Proc. Natl. Acad. Sci. USA **92,** 1749–1753.

Bokoch, G.M. (1994). Regulation of the human neutrophil NADPH oxidase by the Rac GTP-binding proteins. Curr. Opin. Cell Biol. **6,** 212–218.

Braam, J., and Davis, R.W. (1990). Rain-, wind-, and touch-induced expression of calmodulin and calmodulin-related genes in Arabidopsis. Cell **60,** 357–364.

Bush, D.S. (1995). Calcium regulation in plant cells and its role in signaling. Annu. Rev. Plant Physiol. Plant Mol. Biol. **46,** 95–122.

Cao, H., Glazebrook, J., Clarke, J.D., Volko, S., and Dong, X. (1997). The Arabidopsis *NPR1* gene that controls systemic acquired resistance encodes a novel protein containing ankyrin repeats. Cell **88,** 57–63.

De Leo, F.R., Yu, L., Burritt, J.B., Loetterle, L.R., Bond, C.W., Jesaitis, A.J., and Quinn, M.T. (1995). Mapping sites of interaction of p47^{phox} and flavocytochrome *b* with random-sequence peptide phage display libraries. Proc. Natl. Acad. Sci. USA **92,** 7110–7114.

De Leo, F.R., Ulman, K.V., Davis, A.R., Jutila, K.L., and Quinn, M.T. (1996). Assembly of the human neutrophil NADPH oxidase involves binding of p67^{phox} and flavocytochrome *b* to a common functional domain in p47^{phox}. J. Biol. Chem. **271,** 17013–17020.

Desikan, R., Hancock, J.T., Coffey, M.J., and Neill, S.J. (1996). Generation of active oxygen in elicited cells of *Arabidopsis thaliana* is mediated by a NADPH oxidase-like enzyme. FEBS Lett. **382,** 213–217.

Doke, N. (1983a). Involvement of superoxide anion generation in the hypersensitive response of potato tuber tissues to infection with an incompatible race of *Phytophthora infestans* and to the hyphal wall components. Physiol. Plant Pathol. **23,** 345–357.

Doke, N. (1983b). Generation of superoxide anion by potato tuber protoplasts during the hypersensitive response to hyphal wall components of *Phytophthora infestans* and specific inhibition of the reaction by suppressors of hypersensitivity. Physiol. Plant Pathol. **23,** 359–367.

Dwyer, S.C., Legendre, L., Low, P.S., and Leto, T.L. (1996). Plant and human neutrophil oxidative burst complexes contain immunologically related proteins. Biochim. Biophys. Acta **1289,** 231–237.

Finegold, A.A., Shatwell, K.P., Segal, A.W., Klausner, R.D., and Dancis, A. (1996). Intramembrane bis-heme motif for transmembrane electron transport conserved in a yeast iron reductase and the human NADPH oxidase. J. Biol. Chem. **271,** 31021–31024.

Gorin, Y., Leseney, A.M., Ohayon, R., Dupuy, C., Pommier, J., Virion, A., and Dème, D. (1997). Regulation of the thyroid NADPH-dependent H_2O_2 generator by Ca^{2+}: Studies with phenylarsine oxide in thyroid plasma membrane. Biochem. J. **321,** 383–388.

Groom, Q.J., Torres, M.A., Fordham-Skelton, A.P., Hammond-Kosack, K.E., Robinson, N.J., and Jones, J.D.G. (1996). *rbohA*, a rice homologue of the mammalian *gp91^{phox}* respiratory burst oxidase gene. Plant J. **10,** 515–522.

Hammond-Kosack, K.E., and Jones, J.D.G. (1997). Plant disease resistance genes. Annu. Rev. Plant Physiol. Plant Mol. Biol. **48,** 575–607.

Harlow, E.D., and Lane, E. (1988). Antibodies: A Laboratory Manual. (Cold Spring Harbor, NY: Cold Spring Harbor Laboratory Press).

Jabs, T., Tschöpe, M., Colling, C., Hahlbrock, K., and Scheel, D. (1997). Elicitor-stimulated ion fluxes and O_2^- from the oxidative burst are essential components in triggering defense gene activation and phytoalexin synthesis in parsley. Proc. Natl. Acad. Sci. USA **94,** 4800–4805.

Justice, J.M., Murtagh, J.J., Jr., Moss, J., and Vaughan, M. (1995). Hydrophobicity and subunit interactions of rod outer segment proteins investigated using Triton X-114 phase partitioning. J. Biol. Chem. **270,** 17970–17976.

Knight, M.R., Campbell, A.K., Smith, S.M., and Trewavas, A.J. (1991). Transgenic plant aequorin reports the effects of touch and cold-shock and elicitors on cytoplasmic calcium. Nature **352,** 524–526.

Kretsinger, R.H. (1996). EF-hands reach out. Nature Struct. Biol. **3,** 12–15.

Kyte, J., and Doolittle, R.F. (1982). A simple method for displaying the hydropathic character of a protein. J. Mol. Biol. **157,** 105–132.

Lamb, C., and Dixon, R.A. (1997). The oxidative burst in plant disease resistance. Annu. Rev. Plant Physiol. Plant Mol. Biol. **48,** 251–275.

Lamb, C.J., Lawton, M.A., Dron, M., and Dixon, R.A. (1989). Signals and transduction mechanisms for activation of plant defenses against microbial attack. Cell **56,** 215–224.

Larsson, C., Widell, S., and Kjellbom, P. (1987). Preparation of high-purity plasma membranes. Methods Enzymol. **148,** 558–568.

Legendre, L., Rueter, S., Heinstein, P.F., and Low, P.S. (1993). Characterization of the oligogalacturonide-induced oxidative burst in cultured soybean (*Glycine max*) cells. Plant Physiol. **102,** 233–240.

Levine, A., Tenhaken, R., Dixon, R., and Lamb, C. (1994). H_2O_2 from the oxidative burst orchestrates the plant hypersensitive disease resistance response. Cell **79,** 583–593.

Lister, C., and Dean, C. (1993). Recombinant inbred lines for mapping RFLP and phenotypic markers in *Arabidopsis thaliana.* Plant J. **4,** 745–750.

Maruyama, K., Mikawa, T., and Ebashi, S. (1984). Detection of calcium binding proteins by ^{45}Ca autoradiography on nitrocellulose membrane after sodium dodecyl sulfate gel electrophoresis. J. Biochem. **95,** 511–519.

Mehdy, M.C. (1994). Active oxygen species in plant defense against pathogens. Plant Physiol. **105,** 467–472.

Murashige, T., and Skoog, F. (1962). A revised medium for rapid growth and bioassays with tobacco tissue cultures. Physiol. Plant. **15,** 473–497.

Royer-Pokora, B., Kunkel, L.M., Monaco, A.P., Goff, S.C., Newburger, P.E., Baehner, R.L., Cole, F.S., Curnutte, J.T., and Orkin, S.H. (1986). Cloning the gene for an inherited human disorder—chronic granulomatous disease—on the basis of its chromosomal location. Nature **322,** 32–38.

Sambrook, J., Fritsch, E.F., and Maniatis, T. (1989). Molecular Cloning: A Laboratory Manual, 2nd ed. (Cold Spring Harbor, NY: Cold Spring Harbor Laboratory Press).

Schindler, U., Menkens, A.E., Beckmann, H., Ecker, J.R., and Cashmore, A.R. (1992). Heterodimerization between light-regulated and ubiquitously expressed *Arabidopsis* GBF bZIP proteins. EMBO J. **11,** 1261–1273.

Segal, A.W., West, I., Wientjes, F., Nugent, J.H.A., Chavan, A.J., Haley, B., Garcia, R.C., Rosen, H., and Scrace, G. (1992). Cytochrome b_{-245} is a flavocytochrome containing FAD and the NADPH-binding site of the microbiocidal oxidase of phagocytes. Biochem. J. **284,** 781–788.

Seiberler, S., Scheiner, O., Kraft, D., Lonsdale, D., and Valenta, R. (1994). Characterization of a birch pollen allergen, *Bet v* III, representing a novel class of Ca^{2+} binding proteins: Specific expression in mature pollen and dependence of patients' IgE binding on protein-bound Ca^{2+}. EMBO J. **13,** 3481–3486.

Shirasu, K., Nakajima, H., Rajasekhar, V.K., Dixon, R.A., and Lamb, C. (1997). Salicylic acid potentiates an agonist-dependent gain control that amplifies pathogen signals in the activation of defense mechanisms. Plant Cell **9,** 261–270.

Taylor, W.R., Jones, D.T., and Segal, A.W. (1993). A structural model for the nucleotide binding domains of the flavocytochrome b_{-245} β-chain. Protein Sci. **2,** 1675–1685.

Tenhaken, R., Levine, A., Brisson, L.F., Dixon, R.A., and Lamb, C. (1995). Function of the oxidative burst in hypersensitive disease resistance. Proc. Natl. Acad. Sci. USA **92,** 4158–4163.

Wallach, T.M., and Segal, A.W. (1997). Analysis of glycosylation sites on gp91^{phox}, the flavocytochrome of the NADPH oxidase, by site-directed mutagenesis and translation *in vitro.* Biochem. J. **321,** 583–585.

Wang, G.-L., Holsten, T.E., Song, W.-Y., Wang, H.-P., and Ronald, P.C. (1995). Construction of a rice bacterial artificial chromosome library and identification of clones linked to the *Xa21* disease resistance locus. Plant J. **7,** 525–533.

Xing, T., Higgins, V.J., and Blumwald, E. (1997). Race-specific elicitors of *Cladosporium fulvum* promote translocation of cytosolic components of NADPH oxidase to the plasma membrane of tomato cells. Plant Cell **9,** 249–259.

Zhu, Q., Chappell, J., Hedrick, S.A., and Lamb, C. (1995). Accurate *in vitro* transcription from circularized plasmid templates by plant whole cell extracts. Plant J. **7,** 1021–1030.